A&A 534, A98 (2011)
DOI: 10.1051/0004-6361/201117629

Astronomy & Astrophysics

Seismic modelling of the β Cephei star HD 180642 (V1449 Aquilae)

C. Aerts[1,2], M. Briquet[1,3,⋆], P. Degroote[1], A. Thoul[4,⋆⋆], and T. Van Hoolst[1,5]

[1] Instituut voor Sterrenkunde, KU Leuven, Celestijnenlaan 200D, 3001 Leuven, Belgium
e-mail: conny@ster.kuleuven.be
[2] Department of Astrophysics, IMAPP, Radboud University Nijmegen, PO Box 9010, 6500 GL Nijmegen, The Netherlands
[3] LESIA, Observatoire de Paris, CNRS, UPMC, Université Paris-Diderot, 92195 Meudon, France
[4] Institut d'Astrophysique et de Géophysique, Université de Liège, Allée du 6 Août 17, 4000 Liège, Belgium
[5] Royal Observatory of Belgium, Ringlaan 3, 1180 Brussels, Belgium

Received 5 July 2011 / Accepted 19 August 2011

ABSTRACT

Context. We present modelling of the β Cep star HD 180642 based on its observational properties deduced from CoRoT and ground-based photometry as well as from time-resolved spectroscopy.
Aims. We investigate whether present-day state-of-the-art models are able to explain the full seismic behaviour of this star, which has extended observational constraints for this type of pulsator.
Methods. We constructed a dedicated database of stellar models and their oscillation modes tuned to fit the dominant radial mode frequency of HD 180642, by means of varying the hydrogen content, metallicity, mass, age, and core overshooting parameter. We compared the seismic properties of these models with those observed.
Results. We find models that are able to explain the numerous observed oscillation properties of the star, for a narrow range in mass of 11.4–11.8 $M_\odot$ and no or very mild overshooting (with up to 0.05 local pressure scale heights), except for an excitation problem of the $\ell = 3$, p_1 mode. We deduce a rotation period of about 13 d, which is fully compatible with recent magnetic field measurements. The seismic models do not support the earlier claim of solar-like oscillations in the star. We instead ascribe the power excess at high frequency to non-linear resonant mode coupling between the high-amplitude radial fundamental mode and several of the low-order pressure modes. We report a discrepancy between the seismic and spectroscopic gravity at the 2.5σ level.

Key words. stars: oscillations – stars: early-type – stars: massive – asteroseismology – stars: individual: HD 180642 (V1449 Aql) – stars: interiors

1. Introduction

Space asteroseismology started with observations by the small satellites WIRE (Buzasi 2004) and MOST (Matthews 2007). More recently, high-precision time-resolved space photometry has been obtained by the ongoing missions CoRoT (Baglin et al. 2006; Auvergne et al. 2009) and *Kepler* (Burocki et al. 2010; Gilliland et al. 2010) providing significant progress in particular subfields of asteroseismology. Notable discoveries have been made of oscillation properties unknown prior to the era of space asteroseismology for solar-like oscillations, not only in both FGK-type main-sequence stars (e.g., Michel et al. 2008; Chaplin et al. 2011) and red giants (e.g., De Ridder et al. 2009; Beck et al. 2011; Bedding et al. 2011), but also in a massive O-type star (Degroote et al. 2010b).

Thanks to the continuity between space- and ground-based observations, the discovery of hybrid pulsators in various evolutionary stages, i.e., stars pulsating in pressure (p) and gravity (g) modes simultaneously, will also shed new light on the details of stellar structure models. While a few of these hybrid pulsators had been known prior to the space missions, large amounts of them were found from the space photometry, all along the main sequence from spectral type B (e.g., Balona et al. 2011) to F (Grigahcène et al. 2010). Seismic diagnostics suitable for interpreting these cases in terms of modes probing both the core region and the outer envelope are yet to be developed, but it is clear that the numerous gravity modes offer a unique opportunity to test the physics in the deep interior regions adjacent to the core. Initial efforts to explore this region concluded that the input physics of the current models has to be improved to accurately describe chemically inhomogeneous regions in order to be compliant with the space data (Degroote et al. 2010a).

For the most massive pulsators of spectral types O and B0–2, space photometry so far provided more questions than answers. While the detection of pulsations in photometric data was finally established for O-type stars, there seems to be a different cause of the pulsations. The O9V star HD 46202 behaves in a similar way to known β Cep stars (e.g., Aerts et al. 2010, for an extensive overview of all types of pulsators across the Hertzsprung-Russell diagram) but none of its modes is predicted to be excited by the theory that is able to explain the β Cep instability strip (Briquet et al. 2011). Moreover, the O8.5V star HD 46149 appears to oscillate in stochastic modes fulfilling scaling laws and échelle diagrams with clear ridges for modes of equal degree but consecutive radial orders as those observed for Sun-like stars (Degroote et al. 2010b). This implies that this star must have an outer convection zone of considerable size, a suggestion made for massive stars in general, independently of seismic data, from theoretical work (Cantiello et al. 2009). Three hotter O stars do not show any coherent classical pulsational signal, but rather an excess power at low frequency resembling red noise (Blomme et al. 2011). More accurate knowledge of the physics

⋆ Postdoctoral Fellow of the Fund for Scientific Research, Flanders.
⋆⋆ Chercheur Qualifié, FRS-FNRS, Belgium.

in the outer envelope of O stars is needed to understand the variability behaviour detected from CoRoT (there are no O stars in the *Kepler* FoV).

Few B0–2 pulsators with or without emission lines have been observed by CoRoT, while most of the B/Be stars monitored by *Kepler* are cooler. A remarkable finding is the outburst signal detected in the B0.5IVe star HD 49330 (Huat et al. 2009), a phenomenon that has not been observed to occur in any of the other observed Be stars, which are of later spectral type. Theoretical work is needed to understand and interpret the observed frequency patterns in the Be pulsators (Neiner et al. 2009; Diago et al. 2009; Gutiérrez-Soto et al. 2009). Progress is hampered by the mathematical complexity of describing the oscillations in these flattened stars, induced by their rapid rotation, often close to their critical velocity.

To date CoRoT has observed two slow rotators without emission lines situated in the β Cep instability strip. The star B0.5V star HD 51756 turned out to be a rotational modulation variable rather than a pulsator (Pápics et al. 2011). In this work, we present seismic modelling of the only known β Cep class member monitored by CoRoT: the B1.5II-III star HD 180642 (V1449 Aql).

Table 1. Frequencies and mode identification of the highest amplitude modes of HD 180642.

Frequency (d^{-1})	MI method	ℓ	m	i (°)	V_{eq} (km s^{-1})
5.48694	ampl.ratios	0	0		
7.35867	ampl.ratios	0 or 3			
8.40790	LPVs	3	±2	82	38
	or	3	±1	31	78
	or	1	±1	15	119
	or	2	±1	14	104
	or	2	±1	76	26
	or	2	±2	48	52
	or	3	±3	67	26
6.14336	none	...	...	...	...
6.26527	none	...	...	...	...
6.32482	none	...	...	...	...
7.10353	none	...	...	...	...
7.25476	none	...	...	...	...
8.77086	none	...	...	...	...
0.29917	none	...	...	...	...
0.89870	none	...	...	...	...

Notes. MI method can be any of: photometric amplitude ratios (ampl.ratios), line-profile variations (LPVs), not available (none).

2. Summary of observational constraints

The β Cep class member HD 180642 has a visual magnitude of 8.3 and a dominant radial mode with V amplitude 39 mmag (Aerts 2000). The additional observational characteristics of HD 180642 we used as input for the seismic modelling were taken from Degroote et al. (2009, Paper I) and Briquet et al. (2009, Paper II). Paper I was devoted to the analysis of the CoRoT light curve of the star. Three versions of a model description for the light curve were considered: one with classical prewhitening producing 127 significant frequencies, one with harmonics and combination frequencies of 11 independent frequencies, and one where time-dependent amplitudes and phases were allowed. After careful statistical evaluation taking into account penalties for the number of free parameters, the best fit to the CoRoT light curve was found to be the model based on 33 frequencies among which 11 were independent ones (which are repeated in Table 1), 3 were harmonics of the dominant frequency and 19 were combination frequencies (listed in Table 2 of Paper I and not repeated here).

The list of nine highest-amplitude independent stable frequencies contains the one of the dominant radial mode known prior to the CoRoT launch (Aerts 2000), eight frequencies in the range $[6.1, 8.5]\,d^{-1}$, and two frequencies below $1\,d^{-1}$, which could either be due to g modes or connected to the rotation of the star (or both) and agree to within a factor three.

These ten frequencies have amplitudes roughly between 0.8 and 6 mmag (Paper I), i.e., far below the 39 mmag of the dominant mode. The frequency spectrum was found to be atypical of a β Cep star, in the sense that ten sum and nine difference frequencies were also detected, in addition to three harmonics of the dominant frequency. Moreover, several of the combination frequencies were found to have locked phases, a characteristic expected for modes undergoing non-linear mode interaction with the large-amplitude dominant oscillation. The 11 independent largest-amplitude frequencies found in the space photometry are listed in Table 1, along with their mode identification obtained by Aerts (2000) and in Papers I and II. In this work, we consider the nine highest frequencies in that table for the modelling procedure, i.e., the two frequencies below $1\,d^{-1}$ are not used. The total range of frequencies related to dominant independent modes and their combinations covers $[0.3, 27.5]\,d^{-1}$.

In addition to these 33 frequencies, variations with time-dependent behaviour were found in the residual light curve, within the frequency range of the harmonics and the combination frequencies of the heat-driven modes (Belkacem et al. 2009; Paper I). Belkacem et al. (2009) determined a frequency spacing of $1.17\,d^{-1}$ for the range above $11.23\,d^{-1}$ and below $26\,d^{-1}$ and interpreted it in terms of solar-like oscillations caused by stochastic forcing due to convective motions in the outer stellar layers. In Paper I, a value for candidate frequency spacings was recomputed over the range $[4.32, 25.9]\,d^{-1}$ for the three types of prewhitening procedures and led to 1.05, 1.11, and $1.56\,d^{-1}$, with an uncertainty of $\sim 0.02\,d^{-1}$ (the corresponding four spacing values are 13.5, 12.1, 12.9, and 18.0 μHz). The physical interpretation of these spacings remains unclear, given that their value depends on the way the CoRoT light curve is prewhitened. We return to this problem in Sect. 3.7.

In Paper II, we presented the results of an extensive ground-based multicolour photometric and high-resolution spectroscopic campaign that we have organised. This campaign has led to the detection of three of the CoRoT frequencies in the photometry and nine in the spectroscopy, among them the fourth harmonic of the dominant frequency, which is not found in the space photometry. Empirical mode identifation, based on photometric amplitude ratios and on line-profile variability, led to the results in Table 1. In particular, the frequency $7.35867\,d^{-1}$ was identified with either an $\ell = 0$ or $\ell = 3$ mode from amplitude ratios, while the moment method was used to deduce information on the mode wavenumbers (ℓ, m), the inclination angle, and the equatorial velocity for the frequency $8.40790\,d^{-1}$. The seven possibilities listed in Table 1 occurred with a much higher probability than any of the other options for (ℓ, m) and we allow any of those seven solutions in the modelling rather than taking only the best one.

The average spectrum of HD 180642 was also analysed in Paper II to determine the fundamental parameters of the star, as well as its current surface abundance pattern. This resulted in $T_{\rm eff} = 24\,500 \pm 1000$ K, $\log g = 3.45 \pm 0.15$, and

$Z \in [0.0083, 0.0142]$, where the interval for Z covers the dependence on the microturbulent velocity that could not be easily fixed and led to a systematic uncertainty.

We also recall from Paper II that the overall line broadening amounts to 44 km s^{-1}. This is the combined effect of line broadening caused by the projected rotation velocity and the pulsations. It is thus an upper limit to $v \sin i$. The dominant mode has a radial-velocity amplitude of 39 km s^{-1} (Paper II), which, taking into account limb-darkening effects, translates the overall broadening value into an upper limit of $\sim$30 km s^{-1} for $v \sin i$.

Finally, we point out that Hubrig et al. (2011) obtained and analysed spectropolarimetric time series observations taken with the SOFIN échelle spectrograph at the 2.56 m Nordic Optical Telescope, after the discovery of a magnetic field in the star (Hubrig et al. 2009). From their 13 data points, three dominant peaks emerged in the periodogram, with the highest peak at 0.072 d^{-1}. This periodicity was interpreted in the framework of a rigid rotator model for which the period of the magnetic field variation corresponds to a stellar rotation period of 13.9 d, assuming a centred dipole.

3. Modelling procedure

The frequencies above 1 d^{-1} listed in Table 1 are typical of the low-order p and g modes in β Cep stars (e.g., Aerts et al. 2010). The rotation period deduced from the magnetic field measurements combined with realistic values for the radius of a β Cep star lead to equatorial surface rotation velocities that are low relative to the critical velocity. Ignoring the effects of rotation in computing evolutionary models and their oscillation frequencies for the low-order zonal modes is justified in this situation. In practise, this means that we ignore the terms proportional to the square of the rotation frequency in all the equations, including that of hydrostatic support.

For the stellar modelling, we followed a procedure similar to the one adopted by Ausseloos et al. (2004) but for an updated and more extensive grid of models. The latter was computed with the Code Liégeois d'Évolution Stellaire (CLÉS, Scuflaire et al. 2008a), using the input physics described in Briquet et al. (2011) which is not repeated here. An extensive evolutionary model grid covering the entire core-hydrogen burning phase along the main sequence (MS), i.e., from the zero-age main-sequence (ZAMS) to the terminal-age main-sequence (TAMS), for masses M from 7.6 $M_\odot$ to 20.0 $M_\odot$ in steps of 0.1 $M_\odot$, hydrogen mass fractions X from 0.68 to 0.74 in steps of 0.02, metallicities Z from 0.010 until 0.018 in steps of 0.002 and core overshooting parameters $\alpha_{\rm ov}$ between zero and 0.5 in steps of 0.05 (expressed in local pressure scale heights) were considered. The probability of catching the star beyond the TAMS, i.e., in the Hertzsprung gap, is so low that it is not necessary to consider hydrogen-shell burning models. For each of the MS models along the 27 500 tracks, a theoretical oscillation frequency spectrum ignoring the effects of rotation, $\nu_{n\ell}$, was computed in the adiabatic approximation with the code LOSC (Scuflaire et al. 2008b), covering the range of the low-order (typically up to $n = 7$) p and g modes of degree from $\ell = 0$ up to $\ell = 4$.

Following Ausseloos et al. (2004), we did not restrict the model parameters a priori by imposing limits derived from classical spectroscopy, because discrepancies between the seismically and spectroscopically derived fundamental parameters have been reported for a few massive stars in the literature, in particular for the gravity (e.g., Briquet et al. 2007; for the β Cep star θ Oph and Briquet et al. 2011; for the O9V-type pulsator HD 46202). Hence, we instead used the spectroscopic information as a posteriori constraints, after having fitted the nine highest frequencies listed in Table 1.

In the following, we considered models able to fit the dominant radial mode frequency, after which we continued with those for which this mode is excited. For the surviving models, we then required that the additional frequencies higher than the dominant mode frequency be fitted as well. Next, we considered the models fulfilling all these requirements, as well as the constraint on the observed effective temperature. Finally, we also took into account the excitation of the modes in the frequency range [5, 9] d^{-1}.

3.1. Fitting the dominant radial mode frequency

In an initial step, we screened each evolutionary track $(M, X, Z, \alpha_{\rm ov})$ from the ZAMS to the TAMS to find two consecutive models whose radial modes of a particular order encompass the observed frequency of 5.48694 d^{-1}. We considered all pairs of consecutive models that explain the dominant mode as the fundamental or up to the fourth overtone.

For each of those five paired models along the tracks that fulfil this basic requirement, we subsequently computed additional models with a smaller time step to produce one model fitting exactly the frequency of the dominant radial mode, thereby fixing the age, or equivalently, the effective temperature, for that combination of $(M, X, Z, \alpha_{\rm ov}, n)$. In this way, we ended up with some 55 000 models matching the dominant frequency. These are roughly equally distributed over all the considered radial orders n.

For the seismically modelled β Cep stars with a radial mode reported in the literature, this mode was either assumed to be the fundamental or first overtone, or higher overtones were ruled out because they were not compatible with the effective temperature or the gravity of the star. Here, we are dealing with a star whose spectroscopic gravity was determined to be lower than the one of all those previously modelled stars ($\log g = 3.45$). Hence, we did not place any limits on the overtone when interpreting the dominant mode at this stage because we might be dealing with a higher overtone if the star is more evolved than usual for β Cep stars.

3.2. Requesting mode excitation for the dominant mode

The oscillations of the β Cep stars are in general understood in terms of a heat mechanism active in the partial ionisation zones of iron-group elements (Moskalik & Dziembowksi 1992). While the majority of detected and well-identified low-order p and g modes is predicted to be excited by non-adiabatic oscillation computations, some excitation problems occurred and remain to be solved for a few well-established observed non-radial mode frequencies, notably the $\ell = 1$, p_2 modes of the stars ν Eri (Pamyatnykh et al. 2004) and γ Peg (Handler et al. 2009; Zdravkov & Pamyatnykh 2009). To excite these modes in the models, one would need to increase the opacities of iron-group elements. In addition, the predicted frequency of this $\ell = 1$, p_2 mode for appropriate models was found to be shifted with respect to the observed value for both ν Eri and γ Peg. A similar excitation problem occurred for the star 12 Lac (Dziembowski & Pamyatnykh 2008; Desmet et al. 2009).

Theory explains the excitation of the observed radial and p_1 non-radial modes well for the case studies of seismically modelled β Cep stars, except for the very massive ($M \simeq 24\,M_\odot$) O9V pulsator HD 46202, for which none of the detected frequencies is predicted to be excited (Briquet et al. 2011). In particular, the detected radial modes of *all* seismically modelled β Cep stars of spectral type B agree with excitation predictions for these particular modes. We are therefore justified in insisting that the dominant mode of HD 180642 be excited in present-day theoretical computations. To use this requirement as an additional constraint in our stellar modelling, we performed non-adiabatic computations for the radial modes of all the ~55 000 selected models discussed in the previous section with the code MAD (Dupret 2001; Dupret et al. 2002).

For ~18 850 of the models that fit the frequency $5.48694\,\mathrm{d}^{-1}$ as a radial mode, this mode is predicted to be excited. The distribution over the various overtones is as follows: 9964 models have the dominant mode excited as fundamental, 6681 as first overtone, 892 as second overtone, and 1324 as fourth overtone. There are no models with the third overtone excited while there are with an excited fourth overtone. This may seem strange at first sight, but is explained by the occurrence of a resonance of the type $\omega_{p_4} \simeq 2\omega_{p_1}$. It was already known that a resonance $\omega_{p_6} \simeq 3\omega_{p_1}$ occurs in polytropic models (Van Hoolst 1996). Near-resonances were also found in that study, in particular the one we also find here on the basis of more realistic models (Fig. 9 in Van Hoolst 1996). In all the models with the fourth overtone excited, covering the mass interval $[16.3, 20]\,M_\odot$, we also found the fundamental mode at $2.74\,\mathrm{d}^{-1}$ (and quite often also the first overtone) to be excited. This frequency does not occur among the 127 dominant frequencies of HD 180642. These high-overtone models are more evolved and in closer agreement with the spectroscopic $\log g$ than the models with the fundamental mode interpretation.

3.3. Matching the additional non-radial mode frequencies

In the subsequent steps of the modelling procedure, we could not rely on a unique (ℓ, m) identification of the modes corresponding to the observed frequencies, as only limited additional information is available (see Table 1). Moreover, the additional modes all have much lower amplitudes than the one of the dominant mode, thus we did not prefer one above the other for the matching procedure. Thus we requested at once that all eight additional frequencies listed in Table 1 were fitted by model frequencies.

We also imposed that the identification of the degree of the mode with frequency $7.35867\,\mathrm{d}^{-1}$ is fulfilled ($\ell = 0$ or 3). It turned out that this frequency is not a higher overtone radial mode. For the frequency $8.40790\,\mathrm{d}^{-1}$, we requested it to have one of the seven (ℓ, m) combinations listed in Table 1. For each of those possibilities for (ℓ, m), we used the rotational splitting along with the $V_{\rm eq}$ value listed in Table 1 and model radius to deduce the shift in mode frequency implied by rotation, according to the formula

$$\nu_{n\ell m} = \nu_{n\ell 0} + \left(m\,\beta_{n\ell}\,\frac{V_{\rm eq}}{2\pi R} \times 86\,400 \right) \mathrm{d}^{-1} \qquad (1)$$

(e.g., Aerts et al. 2010, Chap. 3), i.e., we limited the frequency matching procedure to first-order effects in the rotation frequency, which is consistent with our grid of spherically-symmetric evolutionary models.

In the matching procedure, we screened all the models which excite and fit the dominant radial mode as described in the previous section and fulfilling all the information in Table 1 for the eight additional measured frequencies, after shifting them according to Eq. (1) and Table 1. The quality of the frequency matching was evaluated by the computation of a reduced χ^2 statistic, where we used $0.02\,\mathrm{d}^{-1}$ as the error for all the eight frequencies because it is a typical uncertainty on theoretically predicted frequencies for non-rotating main sequence pulsators due to differences in the input physics of the models (e.g., Moya et al. 2008). We then considered only those models with $\chi^2 < 1$ and for which each individual frequency is fitted to better than $0.04\,\mathrm{d}^{-1}$. The latter constraint was adopted to avoid a rather large mismatch leading to $\chi^2 < 1$.

In total, 2541 models survived our stringent matching constraints, covering a mass range of $[8.1, 19.9]\,M_\odot$. Among those, some 1000 predict that the dominant frequency is the fundamental mode, some 1200 that it is instead the first overtone and a few hundred that it is either p_3 or p_5.

Six prototypical examples of schematic frequency spectra are shown in Fig. 1. The four that fit the dominant mode as the radial fundamental, predict that the $8.4\,\mathrm{d}^{-1}$ frequency is an $\ell = 2, m = +1$ mode and that the star has an equatorial rotation velocity of $26\,\mathrm{km\,s}^{-1}$. In the case of the first overtone model for the dominant mode, the $8.4\,\mathrm{d}^{-1}$ is an $\ell = +m = 1$ mode for an equatorial rotation of $119\,\mathrm{km\,s}^{-1}$, and in case of the fourth overtone model, the $8.4\,\mathrm{d}^{-1}$ is an $\ell = +m = 2$ mode for a rotation velocity of $52\,\mathrm{km\,s}^{-1}$. As can be seen from Fig. 1, all those cases give a good explanation of the observed frequencies. We stress that these are only six out of many good solutions.

We point out that our procedure was not ideal for the three options for $8.40790\,\mathrm{d}^{-1}$ with the highest equatorial rotation velocity listed in Table 1, for which second-order rotational effects may come into play at a level that can reach values above the theoretical uncertainty we adopted. The estimate of the rotation period from the magnetic field study by Hubrig et al. (2011) would have allowed us to drop these three options from the start. We preferred not to do so, however, as the derivation of the rotation period by Hubrig et al. relies on the assumption of dealing with a rigid rotator model and a centred dipole. While this is a very plausible assumption, and certainly the most obvious one to make, we wanted the seismic modelling to be as independent as possible of this result. This implies that our modelling is not optimal for those three options with high $V_{\rm eq}$, because we did not consider second-order effects in the rotation when computing the evolutionary models and the pulsation frequencies. Improving this would require a full two-dimensional treatment of the equilibrium models and their frequencies, which is beyond the scope of this paper.

3.4. Constraints imposed by spectroscopy

There has been good agreement between spectroscopically derived effective temperatures and abundances, and their seismically derived counterparts, from the method of frequency matching that we adopted here. This is not necessarily the case for the gravity of the seismically modelled β Cep stars. While good agreement was found for several stars (e.g., HD 129929, Dupret et al. 2004; 12 Lac; Desmet et al. 2009), the spectroscopic $\log g$ turned out to be 0.15 dex higher than the seismic $\log g$ for the star θ Oph (Briquet et al. 2007). For HD 46202, the discrepancy even amounted to 0.24 dex (Briquet et al. 2011). Given these previous discrepancies, we prefer not to impose the spectroscopic gravity as a secure constraint in the modelling; this would imply that the dominant mode is a high overtone ($n \geq 3$) while we consider this unlikely. Similarly, the current metallicity of the star measured at its surface is not necessarily the initial one when the

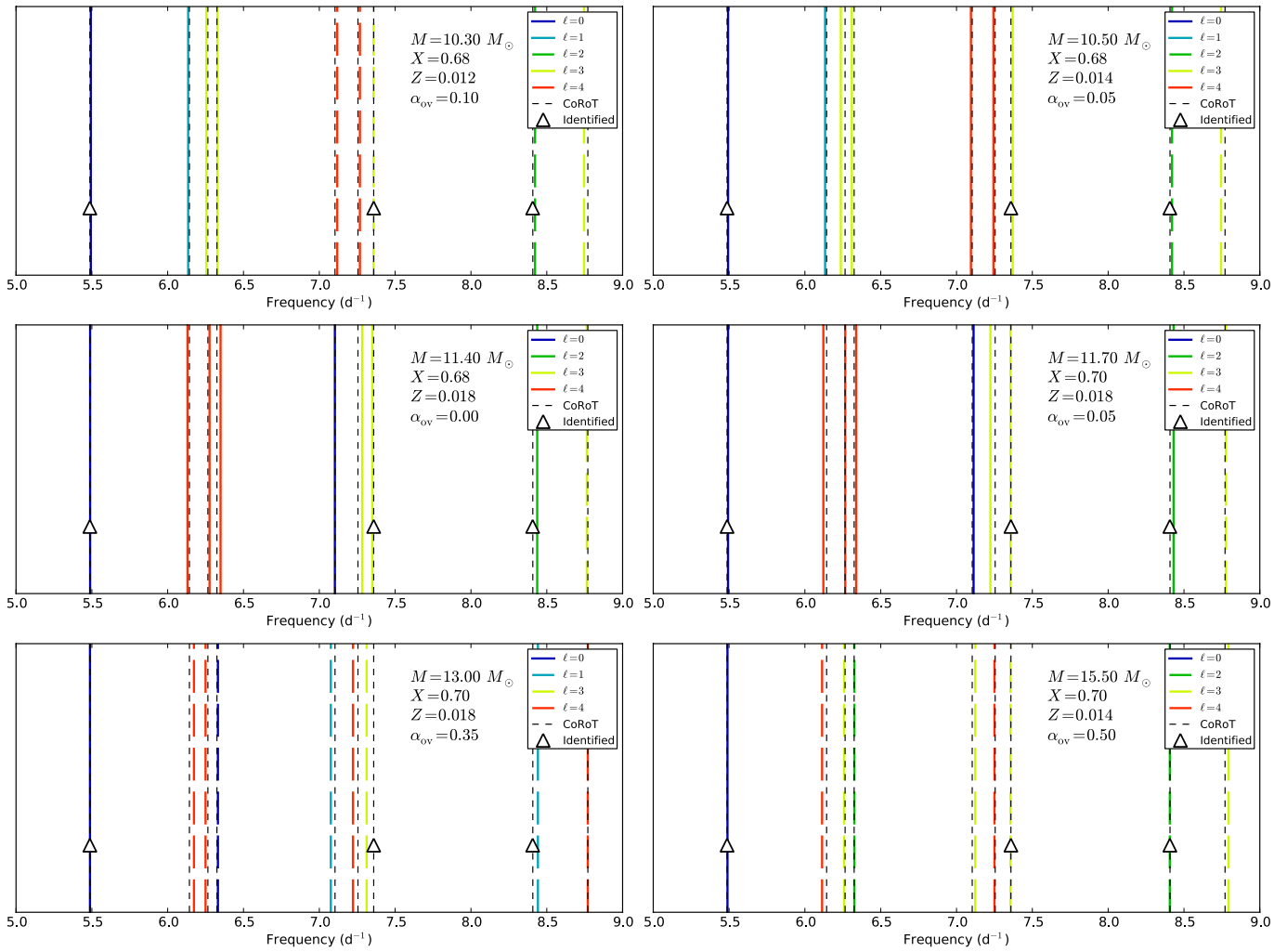

Fig. 1. Models with predicted oscillation frequencies fitting the nine detected frequencies and fulfilling the mode identification as listed in Table 1. In the *four upper panels*, the dominant mode is the radial fundamental while in the *lower left panel* it is the first overtone and in the *lower right panel* the fourth overtone. Full coloured lines indicate excited modes while dashed coloured lines indicate stable modes.

star was born, as effects such as atomic diffusion or unknown mixing may have occurred. Thus, we take a conservative attitude and request as an additional constraint from spectroscopy that the models must fulfil the 1σ error bar in the effective temperature only.

In Fig. 2, all 2541 models surviving the previous section are shown, along with the spectroscopically determined error box in the Kiel diagram. As can be seen, only two models would survive, if we were to impose the 1σ error bar for the gravity of the star. For these two models, none of the observed non-radial modes is excited (see the following section). We consider this too restrictive and continued with all the models that fulfil $T_{\rm eff} \in [23\,500, 25\,500]$ K. There are 357 models left after this requirement, with a mass coverage from 9.5 $M_\odot$ to 15.6 $M_\odot$. This set of models still covers the entire considered range of values for the metallicity, hydrogen fraction, and core overshooting.

3.5. Excitation of the non-radial modes

We subsequently checked the mode excitation of the low-order zonal frequencies for the 357 surviving models with the code `MAD`. Depending on the model parameters, we found excitation for the first radial overtone near frequency 7.1 d^{-1} for masses between 9.7 and 13 $M_\odot$, for the $\ell = 1$, p_1 mode with frequency in $[6.0, 6.5]$ d^{-1} for masses between 9 and 11 $M_\odot$, and for the $\ell = 2$ f mode with frequency near 6.9 d^{-1} for masses between 9.4 and 11.6 $M_\odot$. For $\ell = 3$ and $\ell = 4$, the g_1 modes also have their frequency in $[6.0, 6.5]$ d^{-1} and are found to be excited for masses between 9 and 12 $M_\odot$ while the $\ell = 3$ f mode has its frequency near 7.35 d^{-1} and is excited for masses between 9.7 and 12.2 $M_\odot$. These rough conclusions about the mode excitation are in qualitative agreement with the results on mode excitation found by Dziembowski & Pamyatnykh (2008), but these authors considered only a few representative models that have frequency spectra similar to those observed for the β Cep stars ν Eri and 12 Lac, while we considered an entire grid of models.

To constrain the parameters space for HD 180642, we first eliminated the models for which none of the non-radial modes with frequency above that of the dominant radial mode is excited. This reduced the number of models to 221 and led to an upper limit in mass of 14.1 $M_\odot$. In particular, this removed the two models with the fourth overtone as a fit to the dominant frequency. Only five models able to predict that the dominant mode is the first overtone remained. All of these have only one non-radial mode excited in the frequency range $[6, 9]$ d^{-1}. In each case, this corresponds to the $\ell = 2$, p_1 mode near 6.2 d^{-1}. This is insufficient to explain the observed frequency spectrum and we

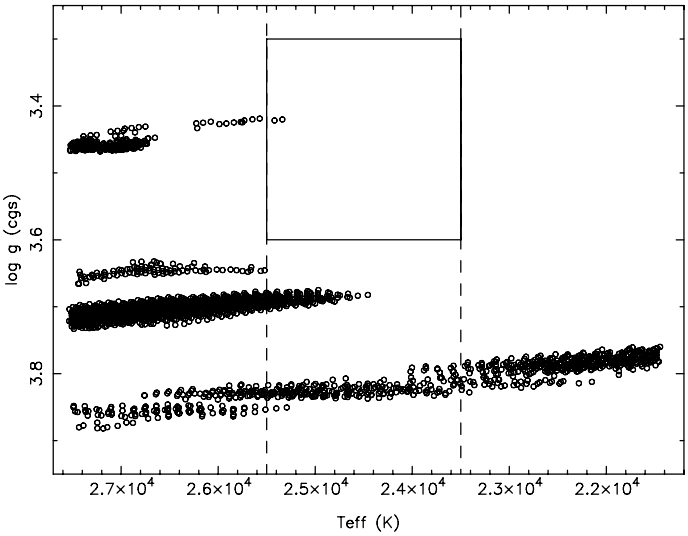

Fig. 2. Kiel diagram showing all the models with a radial mode at the frequency 5.48694 d^{-1} excited and matching the additional eight higher mode frequencies listed in Table 1. The 1σ error box for the spectroscopically derived $T_{\rm eff}$ and log g is shown as well. The dashed vertical lines indicate the restriction we imposed on the models.

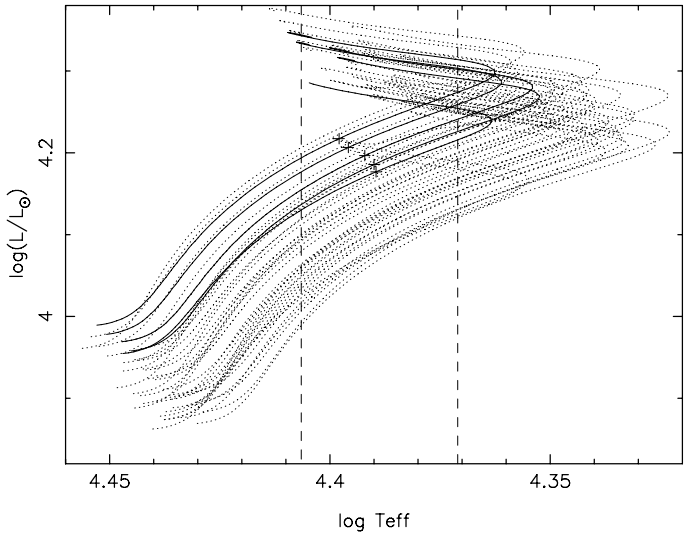

Fig. 3. HR diagram showing the five models listed in the upper part of Table 2 as crosses on their evolutionary track (full lines). These models have excited oscillation modes whose frequencies match all the observed ones, except for the frequency 8.77 d^{-1}, which fits but is predicted to be stable. The 38 dotted tracks each contain one model with excited oscillation frequencies matching the observed ones, except for the two modes with frequency above 8 d^{-1}, which are predicted to be stable.

are thus left with models whose fundamental radial mode fits the dominant frequency.

Among the remaining 221 models, we found five that excite *all but the highest frequency* listed in Table 1. The properties of these five models are listed in the upper part of Table 2. These models are indicated with a cross in Fig. 3 and fulfil the spectroscopically determined effective temperature. The frequency spectra of the two models whose mass is indicated in italics in Table 2 were compared with the observed ones in the middle panels of Fig. 1. Given that excitation problems occur for some modes with frequencies above 7 d^{-1} in the three well-known bright class members ν Eri, 12 Lac, and γ Peg, it is quite encouraging to find models whose oscillation spectra are in full agreement with all the numerous observational constraints, except for the spectroscopic gravity and the excitation of the $\ell = 3$, p_1 mode.

In addition to the five remaining models, there are 38 models for which the mode excitation is fulfilled, except for the two highest frequencies in Table 1, i.e., for one frequency less than the five models in the upper part of Table 2. The evolutionary tracks to which these also "acceptable" models in the lower part of Table 2 belong are indicated as thin dotted lines on Fig. 3, for reference with respect to the five best models. These 43 models together cover a mass range of $[10.5, 12.0]\,M_\odot$, the full range $X \in [0.68, 0.74]$ of the grid, $Z \in [0.014, 0.018]$, and $\alpha_{\rm ov}$ between zero and 0.2. That the initial internal metallicity of the star seems to be somewhat higher (1σ level) than the observed one at the surface for all the acceptable models, might have been introduced by the discrepancy in the gravity, which is not treated independently from the microtubulence in a spectroscopic analysis. It might also be due to effects of diffusion given HD 180642's longitudinal magnetic field of up to 700 G (Hubrig et al. 2009, 2011).

Almost all the seismic models have log $g \simeq 3.83$, which is 0.38 dex (2.5σ) above the best estimate from a classical spectroscopic analysis (Paper II). We thus face another case where the seismic gravity differs from the spectroscopic gravity, just as for the β Cep pulsators θ Oph (B2IV, Briquet et al. 2007) and HD 46202 (O9V, Briquet et al. 2011). Combining the seismic gravity with the equatorial surface rotation velocity of 26 km s^{-1} and a radius of $R \simeq 6.8\,R_\odot$, leads to a surface rotation frequency of 0.075 d^{-1} (rotation period of 13.3 d). We thus find that a factor of four occurs between the surface rotation frequency and the lowest frequency that was jointly detected in the CoRoT light curve and the spectroscopic time series. The frequency 0.89870 d^{-1} listed in Table 1 is 12 times the rotation frequency, within the measurement errors. The seismic rotation period that we obtained from our best-fitting models is in excellent agreement with the most probable period deduced from the magnetic field measurements.

3.6. The full oscillation spectrum

Continuing further with the models in Table 2, we considered their entire oscillation spectrum in the range $[0.2, 40]$ d^{-1}, taking into account all rotational splittings according to the Ledoux formulation (e.g., Aerts et al. 2010) for a rotation frequency of 0.075 d^{-1}, i.e., assuming rigid rotation. In Fig. 4, we show the mode inertia (defined as Eq. (3.140) in Aerts et al. 2010) versus the oscillation frequencies for the seismic model with $M = 11.4\,M_\odot$ listed in Table 2 in the range $[0, 20]$ d^{-1}, for modes with $\ell = 0, \ldots, 4$. We note that the inertia follow a smooth curve as the radial order increases, except for some specific modes of $\ell = 3$ and 4 where the details of the trapping in the interior change owing to the interplay between the mode frequency and the Brünt-Väisälä and Lamb frequencies. The detected frequencies in the best fitting CoRoT light curve model deduced in Paper I are shown as dotted vertical lines, except for the harmonics of the dominant frequency. Full symbols denote modes predicted to be excited from the non-adiabatic computations done with the code `MAD`, while the open symbols are predicted to be stable.

All the combination frequencies (listed in Table 2 of Paper I) in the range $[4, 8.5]$ d^{-1} can be closely identified with frequencies of excited modes. This is also true for the four frequencies

Table 2. Stellar models in agreement with the observational properties of HD 180642.

Mass ($M_\odot$)	Z	α_{ov}	X	$T_{\rm eff}$ (K)	Log g (cgs)	Log $(L/L_\odot)$	R ($R_\odot$)	Age (10^8 yr)	X_c
11.4	0.018	0.00	0.68	24520	3.829	4.177	6.80	0.1243	0.209
11.6	0.018	0.05	0.68	24880	3.832	4.206	6.84	0.1220	0.233
11.7	0.018	0.05	0.68	25000	3.834	4.217	6.86	0.1200	0.235
11.7	0.018	0.05	0.70	24550	3.834	4.186	6.86	0.1296	0.246
11.8	0.018	0.05	0.70	24670	3.835	4.197	6.88	0.1275	0.248
10.5	0.014	0.05	0.68	23880	3.814	4.111	6.64	0.1482	0.182
⋮	⋮	⋮	⋮	⋮	⋮	⋮	⋮	⋮	⋮
12.0	0.018	0.05	0.72	24460	3.837	4.187	6.91	0.1332	0.262

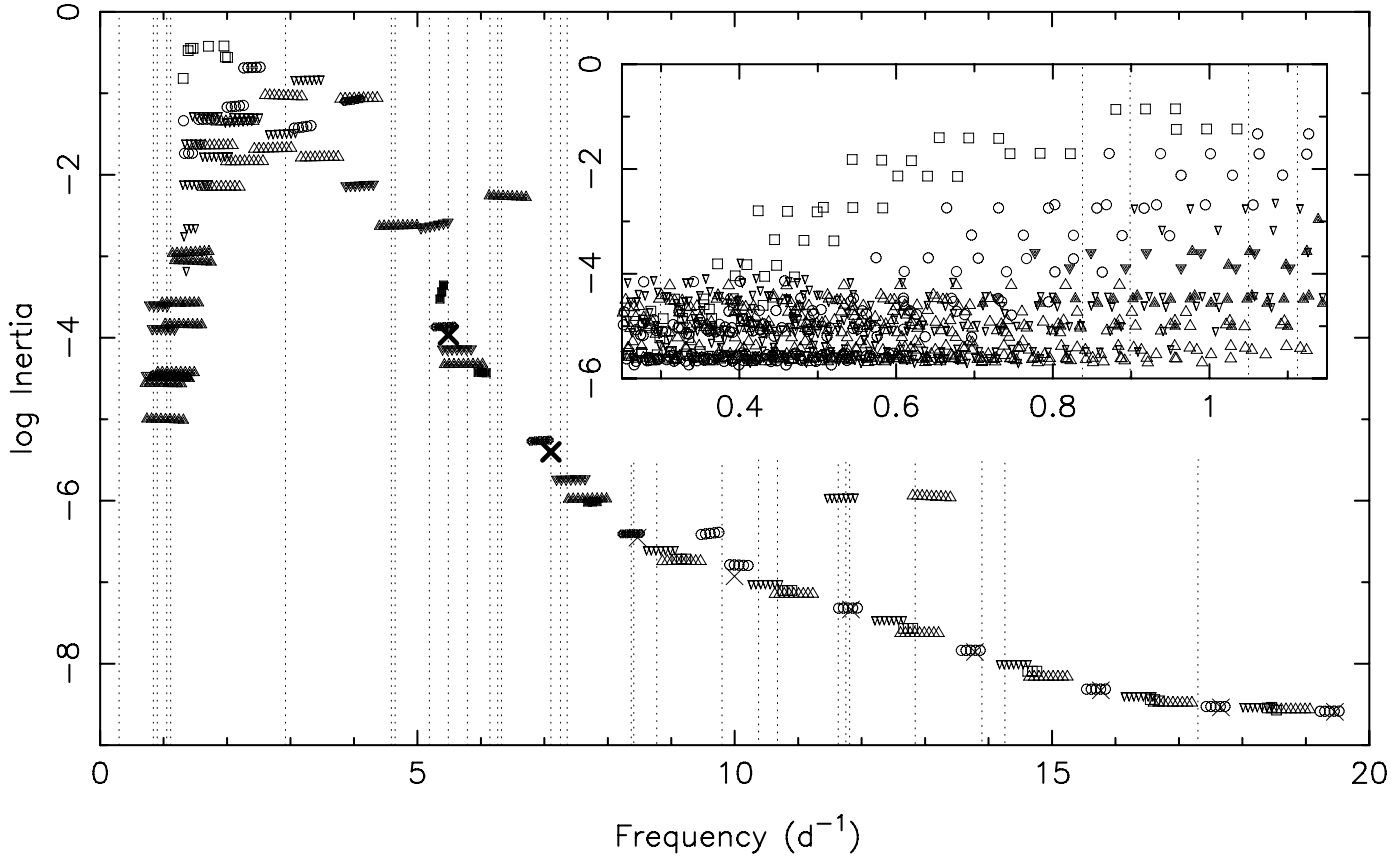

Fig. 4. Mode inertia for the oscillations of the model with $M = 11.4\,M_\odot$, whose other parameters are listed in Table 2. Thick crosses indicate the radial fundamental and first overtone, which are both excited. Thin crosses indicate the higher overtone radial modes, which are not excited. Filled symbols indicate excited non-radial modes and empty symbols stable modes according to the indicated label. The meaning of the symbols is as follows: cross: $\ell = 0$, squares: $\ell = 1$, circles: $\ell = 2$, downward triangle: $\ell = 3$, upward triangle: $\ell = 4$. For clarity, we show only the excited g modes in the region below $1.3\,{\rm d}^{-1}$ in the large panel, while all g modes are shown in the inset. The dotted vertical lines indicate the frequencies detected in the CoRoT light curve (Paper I), nine of which have also been detected in ground-based data (Paper II).

in the range $[0.8, 1.2]\,{\rm d}^{-1}$, which can be explained by excited g modes of intermediate to high radial order (n typically between 10 and 30). All other combination frequencies found in Paper I can be attributed to model frequencies of non-excited p modes taking into account the observational and theoretical uncertainties. If the frequency $0.3\,{\rm d}^{-1}$ were produced by pulsation, it would have to correspond to an $\ell = 3$ mode (Paper II). There are indeed various $\ell = 3$ modes available, taking into account the rotational splitting (see the inset of Fig. 4). These have radial orders from 53 to 60. Given the magnetic field detection for the star, it might also be that this frequency detected in both the photometry and spectroscopy originates from low-amplitude surface inhomogeneities. We are unable to discriminate between these two options. In any case, we interpret the detection of all these modes with combination frequencies that are not excited by the heat mechanism in terms on a non-linear resonant mode excitation by the dominant radial mode, as already proposed in Paper I. That this mechanism seems to be at work and results in frequencies beyond the usual frequency regime of the β Cep stars is supported by the low inertia of these modes (Fig. 4), which makes it much easier to excite them than low-order g modes. The high amplitude of the radial mode thus seems to trigger the excitation of p modes at frequencies between $[8.5, 20]\,{\rm d}^{-1}$, which would otherwise be stable.

The results discussed for the model with $M = 11.4\,M_\odot$ remain qualitatively the same for the four other models listed in the upper part of Table 2.

3.7. Revisiting the case of solar-like oscillations

We used the set of models that fulfil all the seismic requirements of the β Cep-type modes, as well as the combination frequencies, to revisit the claim of solar-like oscillations in the star (Belkacem et al. 2009). In Paper I, the authors already pointed out that the value found for a possible frequency spacing depends on the prewhitening procedure adopted to model the light curve. Moreover, it was found in Paper I that several of the modes with combination frequencies considered by Belkacem et al. (2009), who made their computations for the frequency range $[11, 26]\,\mathrm{d}^{-1}$, are phase-locked, which is not what is expected for stochastic forcing. The interpretation of the residual light curve in terms of solar-like oscillations was also questioned by Balona et al. (2011), in view of the lack of such oscillations in *Kepler* data of B-type pulsators, because these data have higher precision than the CoRoT data. One expects solar-like oscillations in stars with similar fundamental parameters than HD 180642 to have comparable amplitudes, and these amplitudes would be far above the detection limit of *Kepler* data. In the sample of Balona et al. (2011), seven stars have an effective temperature above 20 000 K and are positioned in the joint part of the β Cep and SPB instability strips, but only one of these seven has a temperature close to the one of HD 180642. This star's variability is probably due to rotation and at the mmag level, i.e., a factor of more than ten below the one of our target, so the comparison between the Kepler stars and HD 180642 in terms of solar-like oscillations is premature.

On the observational side, we made an extensive search for ridges in échelle diagrams constructed for the CoRoT residual light curve of HD 180642 discussed in Paper I, adopting the same method as in the case of the CoRoT data of the O8.5V pulsator HD 46149 (Degroote et al. 2010b). In doing so, we considered numerous values for a large frequency spacing. We failed to identify any ridges, in particular also for the value of the spacing reported in Belkacem et al. (2009). This model-independent result stands in contrast to the clear ridges present in the échelle diagram of HD 46149. A comparison between the échelle diagram of HD 46149 and two for HD 180642, one based on the large spacing by Belkacem et al. (2009) and the most likely one reported in Paper I, is shown in Fig. 5. The recently discovered solar-like oscillations in the frequency regime above that of the heat-driven modes in a δ Sct star observed with the *Kepler* satellite did lead to clear ridges in the échelle diagram of that star (Antoci et al. 2011), as is the case for HD 46149.

We then considered our seismic models that explain all the modes of HD 180642 in the frequency regime $[0, 20]\,\mathrm{d}^{-1}$ in terms of heat-driven modes with non-linear mode couplings (listed in Table 2). Irrespective of the cause of the power in the range $[11, 26]\,\mathrm{d}^{-1}$, we first computed all frequency differences between the axisymmetric mode frequencies of consecutive radial order for the same degree ℓ in that interval and compared all these spacing values with the one reported by Belkacem et al. (2009), with an allowed uncertainty of $0.02\,\mathrm{d}^{-1}$. For the model with $M = 11.4\,M_\odot$, this spacing occurs only once, i.e., between the $\ell = 3, m = 0$, g_1 and g_2 modes. It also occurs once between the $\ell = 3, m = 0$, p_3 and p_4 modes of the model with $M = 11.8\,M_\odot$, while it never occurs for the three other models in the upper part of Table 2. Subsequently, we computed all frequency differences for all the axisymmetric modes of $\ell = 0, \ldots, 4$ in the frequency interval $[11, 26]\,\mathrm{d}^{-1}$, to test whether any particular spacing occurred. The outcome of these computations is shown in Fig. 6 for the two models indicated in

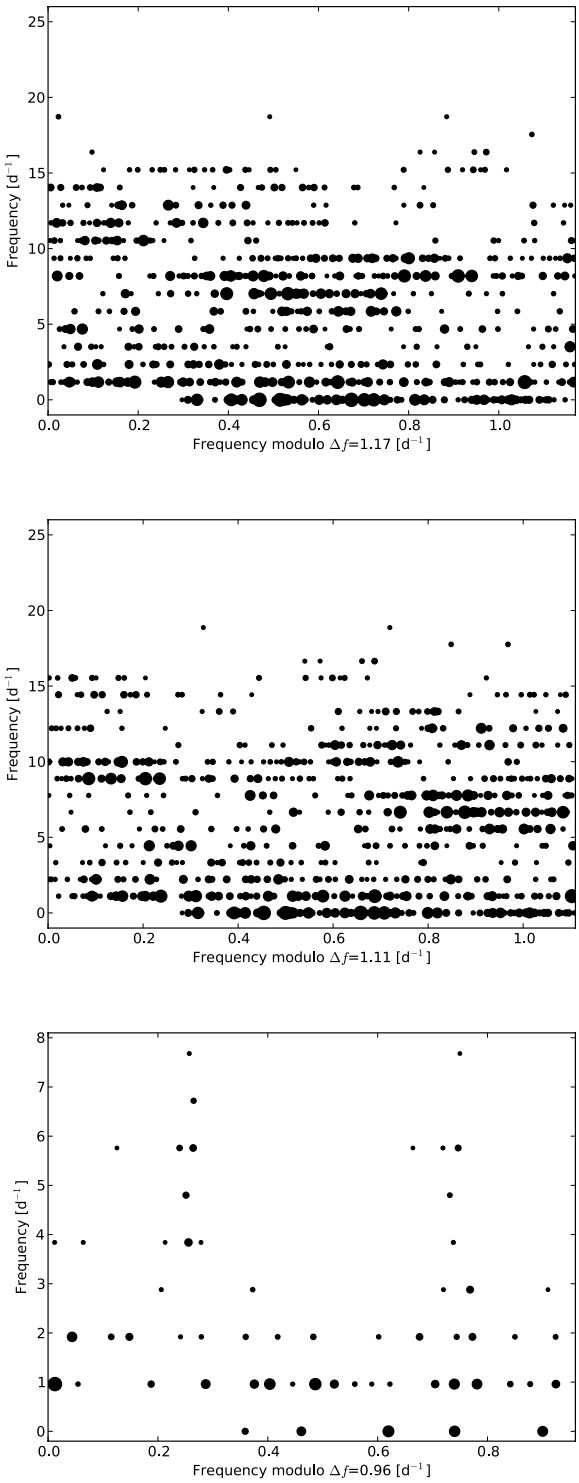

Fig. 5. Échelle diagrams of the CoRoT frequencies for HD 180642 for the large spacing determined by Belkacem et al. (2009, *upper panel*) and in Paper I (*middle panel*). For comparison, we also show the échelle diagram of the O8.5V star HD 46149 reproduced from Degroote et al. (2010b), where clear ridges produced by stochastically excited modes are found. The size of the symbols scales with the power of the frequency.

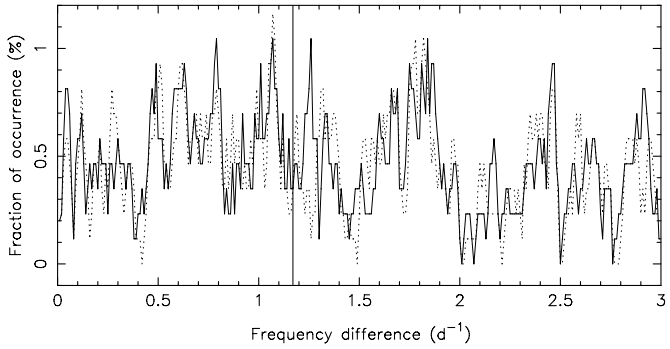

Fig. 6. Fraction of the occurrence of values for the frequency differences between zonal p modes of degree $\ell = 0, \ldots, 4$ in the frequency regime $[11, 26]\,\mathrm{d}^{-1}$ compared with the spacing of $1.17\,\mathrm{d}^{-1}$ reported by Belkacem et al. (2009). The full line is for the model of $11.4\,M_\odot$, while the dotted line is for the model with $11.7\,M_\odot$ indicated in italics in Table 2.

italics in Table 2. It can be seen that no frequency spacing can be discerned among the model frequencies.

4. Concluding remarks

We have managed to explain the extensive observational seismic input deduced from CoRoT and ground-based photometry along with high-resolution spectroscopy of the β Cep star HD 180642 by means of present-day models. All of the 30 detected frequencies are fitted by model frequencies, of which 16 are predicted to be excited and 13 are combination frequencies that can be linked to the dominant radial fundamental mode with an extremely large amplitude for this type of pulsator. Our modelling resulted in a mass between 11.4 and $11.8\,M_\odot$ and a zero or very low core overshooting parameter, along with an age of between 12 and 13 million years (corresponding to a central hydrogen fraction between 0.21 and 0.25) if we allow an excitation problem for only one of the independent oscillation modes, namely for the $\ell = 3$, p_1 mode with a frequency $8.77\,\mathrm{d}^{-1}$. This is a frequency regime where similar excitation problems have been found for this type of pulsator (e.g., Dziembowski & Pamyatnykh 2008; Zdravkov & Pamyatnykh 2009). All other observed frequencies that are not excited by the heat mechanism can be explained as eigenmodes triggered by the large-amplitude radial mode by means of non-linear resonant mode excitation.

We are unable to support the findings of Belkacem et al. (2009) from the seismic models which explain the oscillation spectrum of HD 180642 in the frequency regime $[0, 20]\,\mathrm{d}^{-1}$, i.e., the nature of the power excess in the p-mode frequency regime of HD 180642 is different from the one of "classical" solar-like oscillations caused by the stochastic forcing due to convective motions. We instead attribute the occurrence of time-dependent amplitudes and phases in the frequency regime above the radial fundamental mode to the effect of the non-linear resonant mode coupling which is activated by the large amplitude of the dominant mode. This provides a natural explanation for the lack of detections of solar-like oscillations in B stars monitored by both the CoRoT and *Kepler* missions. All of the B pulsators observed by these satellites indeed have much lower amplitudes (at least by a factor ten below the dominant mode of HD 180642) so resonant mode coupling is not expected for these, while solar-like oscillations would have been detected if they existed in such types of stars.

We find, once more, a discrepancy between the spectroscopic $\log g$ and the seismic $\log g$, as was found before in two other seismically modelled OB stars. We assign this to the systematic uncertainty when deducing $\log g$ from the wings of spectral lines of one snapshot spectrum or from an average of a time series of spectra. In both cases, the pulsational broadening is not taken into account in an appropriate way. Indeed, oscillations change the shape of spectral lines in an asymmetric and time-dependent way, i.e., the level of deformation depends on the phase in the overall oscillation cycle. To compensate for this deformation and absence of pulsational broadening, one usually introduces a time-independent ad-hoc parameter called macroturbulence (e.g., Aerts et al. 2009) and/or a rotational profile with a wrong $v \sin i$, each of which are usually deduced from metal lines and have a different functional shape than the true time-dependent line-broadening function. This is then compensated for by an incorrect value of the gravity and/or microturbulence, which can either be too high or too low. In addition to this, the normalisation of the spectra, which is a necessary manipulation of the data required to deduce the position and shape of the line wings with respect to the continuum, is by no means a trivial operation and in itself introduces systematic uncertainty. In the present case of HD 180642, for instance, the gravity was deduced from four Balmer line wings assuming a rotational profile of $44\,\mathrm{km\,s}^{-1}$, while a problem was encountered in deriving the microturbulence in a consistent way, because a discrepancy of $5\,\mathrm{km\,s}^{-1}$ occurred between the values deduced from the N and O lines for this quantity. Our seismic analysis inferred that $v \sin i = 25\,\mathrm{km\,s}^{-1}$ only. There are thus various uncertainties to be considered for quantities that are not independent. The seismic gravity is a quantity determined by the entire stellar structure, which is very strongly constrained for HD 180642 by the numerous seismic properties measured for this star. In view of the discrepancy, we advise the use spectroscopically derived $\log g$-values of pulsators with a 3σ error bar. Temperature estimates are not affected by this uncertainty as they rely on an ionisation balance of Si for which three stages are available in the case of β Cep stars, hence this quantity is not very dependent on the line shapes.

Acknowledgements. The research leading to these results has received funding from the European Research Council under the European Community's Seventh Framework Programme (FP7/2007–2013)/ERC grant agreement No. 227224 (PROSPERITY), from the Research Council of K.U. Leuven grant agreement GOA/2008/04 and from the Belgian Federal Space Office under contract C90309: CoRoT Data Exploitation. M.B. and C.A. acknowledge the Fund for Scientific Research – Flanders for a grant for a long stay abroad and for a sabbatical leave, respectively.

References

Aerts, C. 2000, A&A, 361, 245
Aerts, C., Puls, J., Godart, M., & Dupret, M.-A. 2009, A&A, 508, 409
Aerts, C., Christensen-Dalsgaard, J., & Kurtz, D. W. 2010, Asteroseismology (Springer)
Antoci, V., Handler, G., Campante, T. L., et al. 2011, Nature, 477, 570
Ausseloos, M., Scuflaire, R., Thoul, A., & Aerts, C. 2004, MNRAS, 355, 352
Auvergne, M., Bodin, P., Boisnard, L., et al. 2009, A&A, 506, 411
Baglin, A., Auvergne, M., Barge, P., et al. 2006, ESASP, 1306, 33
Balona, L. A., Pigulski, A., De Cat, P., et al. 2011, MNRAS, 413, 2304
Beck, P. G., Bedding, T. R., Mosser, B., et al. 2011, Science, 332, 205
Bedding, T. R., Mosser, B., Huber, D., et al. 2011, Nature, 471, 608
Belkacem, K., Samadi, R., Goupil, M.-J., et al. 2009, Science, 324, 1540
Blomme, R., Mahy, L., Catala, C., et al. 2011, A&A, 533, A4
Borucki, W. J., Koch, D., Basri, G., et al. 2010, Science, 327, 977
Briquet, M., Morel, T., Thoul, A., et al. 2007, MNRAS, 381, 1482
Briquet, M., Uytterhoeven, K., Morel, T., et al. 2009, A&A, 506, 269 (Paper II)

Briquet, M., Aerts, C., Baglin, A., et al. 2011, A&A, 527, A112
Busazi, D. L. 2004, ESA SP-538, 205
Cantiello, M., Langer, N., Brott, I., et al. 2009, A&A, 499, 279
Chaplin, W. J., Kjeldsen, H., Christensen-Dalsgaard, J., et al. 2011, Science, 332, 213
Degroote, P., Briquet, M., Catala, C., et al. 2009, A&A, 506, 111 (Paper I)
Degroote, P., Aerts, C., Baglin, A., et al. 2010a, Nature, 464, 259
Degroote, P., Briquet, M., Auvergne, M., et al. 2010b, A&A, 519, A38
De Ridder, J., Barban, C., Baudin, F., et al. 2009, Nature, 459, 398
Desmet, M., Briquet, M., Thoul, A., et al. 2009, MNRAS, 396, 1460
Diago, P. D., Gutiérrez-Soto, J., Auvergne, M., et al. 2009, A&A, 506, 125
Dupret, M.-A. 2001, A&A, 366, 166
Dupret, M.-A., De Ridder, J., Neuforge, C., et al. 2002, A&A, 385, 563
Dupret, M.-A., Thoul, A., Scuflaire, R., et al. 2004, A&A, 415, 251
Dziembowski, W., & Pamiatnykh, A. A. 1993, MNRAS, 262, 204
Gilliland, R. L., Brown, T. M., Christensen-Dalsgaard, J., et al. 2010, PASP, 122, 131
Grigahcène, A. V., Balona, L. A., et al. 2010, ApJ, 713, L192
Gutiérrez-Soto, J., Floquet, M., Samadi, R., et al. 2009, A&A, 506, 133
Handler, G., Matthews, J. M., Eaton, J. A., et al. 2009, ApJ, 698, L56
Hubrig, S., Briquet, M., De Cat, P., et al. 2009, AN, 330, 317
Hubrig, S., Ilyin, I., Briquet, M., et al. 2011, A&A, 531, L20
Huat, A.-L., Hubert, A.-M., Baudin, F., et al. 2009, A&A, 506, 95
Matthews, J. M. 2007, 150, CoAst, 333
Michel, E., Baglin, A., Auvergne, M., et al. 2008, Science, 322, 558
Moskalik, P., & Dziembowski, W. A. 1992, 256, L5
Moya, A., Christensen-Dalsgaard, J., Charpinet, S., et al. 2008, Ap&SS, 316, 231
Neiner, C., Gutiérrez-Soto, J., Baudin, F., et al. 2009, A&A, 506, 143
Pamyatnykh, A. A., Handler, G., & Dziembowski, W. 2004, MNRAS, 350, 1022
Pápics, P. I., Briquet, M., Auvergne, M., et al. 2011, A&A, 528, A123
Scuflaire, R., Théado, S., Montalbán, J., et al. 2008a, Ap&SS, 316, 83
Scuflaire, R., Montalbán, J., Théado, S., et al. 2008b, Ap&SS, 316, 149
Van Hoolst, T. 1996, A&A, 308, 66
Zdravkov, T., & Pamyatnykh, A. A. 2009, in Stellar Pulsation: Challenges for Theory and observations, ed. J. A. Guzik, & P. A. Bradley, AIP Conf. Proc., 1170, 388